The 2010 IEEE/RSJ International Conference on
Intelligent Robots and Systems
October 18-22, 2010, Taipei, Taiwan

Enhanced Operational Space Formulation for Multiple Tasks using Time Delay Estimation

Jae Won Jeong, *Student Member, IEEE*, Pyung Hun Chang, *Member, IEEE, and* Jinoh Lee, *Student Member, IEEE*

Abstract— **In this paper, the practical problems of the Operational Space Formulation (OSF) are considered. The OSF provides decentralized control of the tasks by virtue of the 'dynamic decoupling property'. In the practical view point, however, the OSF can be unfavorable due to the inevitable modeling error and large computational effort. As a remedy for this problem, the OSF is enhanced with Time-Delay Estimation (TDE) scheme. The robustness and efficiency of the proposed control have been analyzed and demonstrated to be effective against the practical problems while preserving the dynamic decoupling property.**

I. Introduction

THE Operational Space Formulation (OSF) [1]-[4] provides the decentralized control of an arbitrary number of tasks in parallel by virtue of the useful property *dynamic decoupling*: the force for one task does not affect the motion of the other tasks [4], [5]. Owing to the physical merit, the OSF has been widely applied to control many robotic systems with consistently good results: multi-arm robotic systems [4], [6], surgery robots [7], and humanoid robots [2], [3]. Especially, the recent results in humanoid robots shed the new light on the natural movement generation of high-degrees-of-freedom robots that is one of the open and interesting problems in the field of robotics.

The OSF, however, can be practically unfavorable in respects of the inevitable modeling error and of the relatively high computational effort [8] as the following.

The OSF requires precise robot dynamics models. In the practical view point, the modeling error is inevitable: the dynamics parameters vary due to the change of the payload, and precise modeling of the friction force is still an open problem. It has been reported that the OSF reveals noticeable performance degradation in the presence of modeling error [8]. One reason is that the modeling error of the inertia creates many sources of errors in the motor commands due to repeated usage of inertia [8]. An accurate model of the inertia is essential for the dynamic decoupling property. Under the modeling error of inertia, the OSF fails to decouple each task-dynamics. A learning method has been proposed as a remedy for modeling error problem [9]. However, the method is complex and computationally burdensome.

The OSF requires relatively large computational effort. The evaluation of explicit dynamic models is computationally demanding. Particularly, inversion of the inertia is the most expensive [8], [10]. An efficient computation algorithm that does not require explicit inversion of the inertia was proposed [10]. However, the algorithm can be applied only for the primary task not for the secondary tasks. The large computational effort of the OSF is still burdensome in spite of recent developments of the computing hardware: the heavy charge of computation requires a large expense for hardware of real-time control, and the high performance hardware lays a burden on the battery-capacity of the mobile robots such as humanoids since it generally consumes large electric power [9].

This paper introduces Time-Delay Estimation (TDE) [11]-[14] to practically enhance the OSF, an OSF with TDE (OSFTDE): *1) robustness for the modeling error* regarding to both the dynamical decoupling and the control performance, and *2) high computational efficiency*. TDE scheme provides an accurate estimate of the complex nonlinear robot dynamics. By virtue of TDE scheme, the dynamic decoupling property is feasible even with a constant nominal model of inertia; good control performance is obtained in face of the modeling error. Also, TDE saves expensive computations in the OSF: nonlinear forces−Coriolis and centrifugal force, gravity force, and friction force−are not required to be computed. The inversion of the inertia, the most expensive computation in the OSF, can be saved since a constant nominal model of inertia can be used and its inverse can be obtained off-line.

The paper is structured as follows: In section II, TDE is briefly reviewed, and the practically enhanced OSF, the OSFTDE, is presented. In section III, the practical advantages of the OSFTDE are analyzed through the comparison with the OSF. Finally, the results are summarized and conclusions are drawn in Section IV.

II. OSFTDE

A. Decoupled Operational Space Dynamics

The rigid-body dynamics equation of robot with n degrees of freedom (DOFs) is given as

$$\mathbf{A}(\mathbf{q})\ddot{\mathbf{q}} + \mathbf{b}(\mathbf{q},\dot{\mathbf{q}}) + \mathbf{g}(\mathbf{q}) + \mathbf{f}(\mathbf{q},\dot{\mathbf{q}}) - \boldsymbol{\Gamma}_e = \boldsymbol{\Gamma}, \quad (1)$$

where $\boldsymbol{\Gamma}, \boldsymbol{\Gamma}_e \in \Re^n$ denote the joint torque and the interaction torque; $\mathbf{q}, \dot{\mathbf{q}}, \ddot{\mathbf{q}} \in \Re^n$ denote the joint angle, the joint velocity,

Manuscript received March 10, 2010. This research was supported by the Ministry of Knowledge Economy, Republic of Korea under the 21st Century Frontier R&D programs and the Daedoek Innopolis R&D programs

The authors are with the Department of Mechanical Engineering, KAIST, Daejeon, Republic of Korea (e-mail: mechjjw@mecha.kaist.ac.kr; phchang@mecha.kaist.ac.kr; and jinoh_lee@mecha.kaist.ac.kr).

and the joint acceleration, respectively; $\mathbf{A}(\mathbf{q}) \in \Re^{n \times n}$ a positive definite inertia, $\mathbf{b}(\mathbf{q}, \dot{\mathbf{q}}) \in \Re^n$ Coriolis and centrifugal torque, and $\mathbf{g}(\mathbf{q}) \in \Re^n$ gravity torque; $\mathbf{f}(\mathbf{q}, \dot{\mathbf{q}}) \in \Re^n$ stands for the friction including Coulomb friction, viscous friction and stiction.

Introducing a constant nominal model of the inertia, $\bar{\mathbf{A}} \in \Re^{n \times n}$, another expression of (1) is obtained as follows:

$$\bar{\mathbf{A}}\ddot{\mathbf{q}} + \mathbf{H}(\mathbf{q}, \dot{\mathbf{q}}, \ddot{\mathbf{q}}) = \boldsymbol{\Gamma}, \tag{2}$$

where $\mathbf{H}(\mathbf{q}, \dot{\mathbf{q}}, \ddot{\mathbf{q}})$ denotes all nonlinear terms as

$$\mathbf{H}(\mathbf{q}, \dot{\mathbf{q}}, \ddot{\mathbf{q}}) = [\mathbf{A}(\mathbf{q}) - \bar{\mathbf{A}}]\ddot{\mathbf{q}} + \mathbf{b}(\mathbf{q}, \dot{\mathbf{q}}) + \mathbf{g}(\mathbf{q}) + \mathbf{f}(\mathbf{q}, \dot{\mathbf{q}}) - \boldsymbol{\Gamma}_{\mathbf{e}}. \tag{3}$$

Note that $\mathbf{H}(\mathbf{q}, \dot{\mathbf{q}}, \ddot{\mathbf{q}})$ represents the difference of two dynamics− linear dynamics, $\bar{\mathbf{A}}\ddot{\mathbf{q}}$, and the other nonlinear dynamics.

Assume that there are k tasks and the i th task has lower priority with respect to the previous $(i-1)$ tasks. The i th task is represented as the coordinate vector, $\mathbf{x}_i(\mathbf{q}) \in \Re^{m_i}$ with the associated Jacobian $\mathbf{J}_i(\mathbf{q}) = \partial \mathbf{x}_i(\mathbf{q}) / \partial \mathbf{q}$.

The OSF describes the torque level decomposition as follows:

$$\boldsymbol{\Gamma} = \boldsymbol{\Gamma}_1 + \boldsymbol{\Gamma}_{2|prev(2)} + \cdots \boldsymbol{\Gamma}_{k|prev(k)}, \tag{4}$$

where $\boldsymbol{\Gamma}_{i|prev(i)} \in \Re^n$ denotes the prioritized torque that does not '*disturb*' the primary task in dynamics level, and the subscript $\bullet_{i|prev(i)}$ indicate that $\bullet$ of the i th task is projected onto the null-space of the previous $(i-1)$ tasks.

Torque vector can be obtained for the operational space force of the i th task, $\mathbf{F}_i \in \Re^{m_i}$, as follows:

$$\boldsymbol{\Gamma}_i = \mathbf{J}_i^T \mathbf{F}_i. \tag{5}$$

Then, the prioritized torque, $\boldsymbol{\Gamma}_{i|prev(i)}$, is obtained by projecting $\boldsymbol{\Gamma}_i$ onto the dynamic-consistent null space of the tasks with the higher priority:

$$\begin{aligned} \boldsymbol{\Gamma}_{i|prev(i)} &= \mathbf{N}_{prev(i)}{}^T \boldsymbol{\Gamma}_i \\ &= \mathbf{N}_{prev(i)}{}^T (\mathbf{J}_i^T \mathbf{F}_i), \\ &= \mathbf{J}_{i|prev(i)}{}^T \mathbf{F}_i \end{aligned} \tag{6}$$

where $\mathbf{N}_{prev(i)} \in \Re^{n \times n}$ denotes the dynamic-consistent null space projector such that

$$(\mathbf{J}_i \bar{\mathbf{A}}^{-1}) \mathbf{N}_{prev(j)}{}^T = \mathbf{0}, \quad \text{for } i < j, \tag{7}$$

and $\mathbf{J}_{i|prev(i)} = \mathbf{J}_i \mathbf{N}_{prev(i)}$ denotes the task-consistent Jacobian of the i th task. The dynamic-consistent null space projector, $\mathbf{N}_{prev(i)}$, is efficiently obtained as follows [3], [15]:

$$\mathbf{N}_{prev(i)} = \mathbf{I} - \sum_{j=1}^{i-1} \mathbf{J}_{j|prev(j)}{}^{\bar{\mathbf{A}}+} \mathbf{J}_{j|prev(j)}. \tag{8}$$

Let the task-consistent operational space acceleration be

$$\ddot{\mathbf{x}}_{i|prev(i)} = \mathbf{J}_{i|prev(i)} \ddot{\mathbf{q}} + \dot{\mathbf{J}}_{i|prev(i)} \dot{\mathbf{q}}. \tag{9}$$

From (2), the joint-acceleration is obtained as

$$\ddot{\mathbf{q}} = \bar{\mathbf{A}}^{-1}[\boldsymbol{\Gamma} - \mathbf{H}(\mathbf{q}, \dot{\mathbf{q}}, \ddot{\mathbf{q}})]. \tag{10}$$

Substituting (4) and (10) into (9) leads to the equation of motion of the i th task as follows:

$$\mathbf{F}_i = \bar{\boldsymbol{\Lambda}}_{i|prev(i)}(\mathbf{q}) \ddot{\mathbf{x}}_{i|prev(i)} + \mathbf{H}_{i|prev(i)}(\mathbf{q}, \dot{\mathbf{q}}, \ddot{\mathbf{q}}), \tag{11}$$

where

$$\bar{\boldsymbol{\Lambda}}_{i|prev(i)}(\mathbf{q}) = [\mathbf{J}_{i|prev(i)}(\mathbf{q}) \bar{\mathbf{A}}^{-1} \mathbf{J}_{i|prev(i)}(\mathbf{q})^T]^{-1}, \tag{12}$$

$$\begin{aligned} \mathbf{H}_{i|prev(i)}(\mathbf{q}, \dot{\mathbf{q}}, \ddot{\mathbf{q}}) = &-\bar{\boldsymbol{\Lambda}}_{i|prev(i)}(\mathbf{q}) \dot{\mathbf{J}}_{i|prev(i)} \dot{\mathbf{q}} \\ &+ (\mathbf{J}_{i|prev(i)}{}^{\bar{\mathbf{A}}+})^T \mathbf{H}(\mathbf{q}, \dot{\mathbf{q}}, \ddot{\mathbf{q}}) \end{aligned}, \tag{13}$$

and

$$\mathbf{J}_{i|prev(i)}{}^{\bar{\mathbf{A}}+} = \bar{\mathbf{A}}^{-1} \mathbf{J}_{i|prev(i)}{}^T \bar{\boldsymbol{\Lambda}}_{i|prev(i)}. \tag{14}$$

Note that $\mathbf{H}_{i|prev(i)}(\mathbf{q}, \dot{\mathbf{q}}, \ddot{\mathbf{q}})$ includes all nonlinear terms of the i th task dynamics.

B. Time-Delay Estimation (TDE)

In this section, $\mathbf{H}_{i|prev(i)}(\mathbf{q}, \dot{\mathbf{q}}, \ddot{\mathbf{q}})$ is to be efficiently and accurately estimated by TDE scheme.

Assume that $\mathbf{H}_{i|prev(i)}(\mathbf{q}, \dot{\mathbf{q}}, \ddot{\mathbf{q}})$ is continuous or at least piece-wise continuous about time t. Then, for a sufficiently small time-delay, L, the time delayed estimate of $\mathbf{H}_{i|prev(i)}(\mathbf{q}, \dot{\mathbf{q}}, \ddot{\mathbf{q}})$ can be obtained as below:

$$\begin{aligned} \hat{\mathbf{H}}_{i|prev(i)}(\mathbf{q}, \dot{\mathbf{q}}, \ddot{\mathbf{q}}) &= \mathbf{H}_{i|prev(i)}(\mathbf{q}, \dot{\mathbf{q}}, \ddot{\mathbf{q}})_{(t-L)} \\ &= \mathbf{F}_{i(t-L)} - \bar{\boldsymbol{\Lambda}}_{i|prev(i)} \ddot{\mathbf{x}}_{i|prev(i)(t-L)} \end{aligned}, \tag{15}$$

where $\hat{\bullet}$ denotes the estimated value of $\bullet$, and $\bullet_{(t-L)}$ denotes time delayed value of $\bullet$. It is noteworthy that TDE does not require a dynamic model or its parameters except for $\bar{\boldsymbol{\Lambda}}_{i|prev(i)}$. It only needs the recent past information of acceleration and input force.

In practice, the smallest achievable L is the sampling period in digital implementation. A digital control system behaves reasonably close to the continuous system if the sampling rate is faster than 30 times the system bandwidth [16]. Hence, with L smaller than this level, $\mathbf{H}_{i|prev(i)}(\mathbf{q}, \dot{\mathbf{q}}, \ddot{\mathbf{q}})$ can be estimated by TDE.

C. Control Based on TDE

The control objective is to yield the decoupled behavior, $\ddot{\mathbf{x}}_i^* = \ddot{\mathbf{x}}_i$, where $\ddot{\mathbf{x}}_i^*$ denotes the reference acceleration for the i th task.

From (4) and (11), the control torque is designed as follows:

$$\boldsymbol{\Gamma} = \mathbf{J}_1^T \mathbf{F}_1 + \mathbf{J}_{2|prev(2)}{}^T \mathbf{F}_2 + \cdots + \mathbf{J}_{k|prev(k)}{}^T \mathbf{F}_k, \tag{16}$$

and

$$\mathbf{F}_i = \underbrace{\bar{\boldsymbol{\Lambda}}_{i|prev(i)}(\mathbf{q})(\ddot{\mathbf{x}}_i^* - \ddot{\mathbf{x}}_{i\_bias})}_{\text{Injecting the desired dynamics}} + \underbrace{\mathbf{F}_{i(t-L)} - \bar{\boldsymbol{\Lambda}}_{i|prev(i)} \ddot{\mathbf{x}}_{i|prev(i)(t-L)}}_{\text{Canceling the nonlinearities}}, \tag{17}$$

where $\ddot{\mathbf{x}}_{i\_bias}$ denotes the bias-acceleration [2], [3]

$$\ddot{\mathbf{x}}_{i\_bias} = \ddot{\mathbf{x}}_{i|prev(i)} - \ddot{\mathbf{x}}_i. \tag{18}$$

The reference accelerations should be assigned in accordance with the objects to be controlled: position, force, or impedance.

In this paper, we adopt the reference accelerations for the impedance control [17]-[19] since: 1) the impedance control provides *desired compliance*[1] for the task that needs to interact with the environment; 2) the impedance control can be general form of *the other controls* [18].

The objective of the impedance control is to make a robot achieve the following target-impedance dynamics:

$$\mathbf{\Lambda}_{id}(\ddot{\mathbf{x}}_{id}-\ddot{\mathbf{x}}_i)+\mathbf{B}_{id}(\dot{\mathbf{x}}_{id}-\dot{\mathbf{x}}_i)+\mathbf{K}_{id}(\mathbf{x}_{id}-\mathbf{x}_i)=\mathbf{F}_{ei}, \quad (19)$$

where $\mathbf{\Lambda}_{id}\in\Re^{m_i\times m_i}$, $\mathbf{B}_{id}\in\Re^{m_i\times m_i}$, and $\mathbf{K}_{id}\in\Re^{m_i\times m_i}$ denote the desired inertia matrix, desired damping matrix, and desired stiffness matrix, respectively; $\ddot{\mathbf{x}}_{id}$, $\dot{\mathbf{x}}_{id}$, and $\mathbf{x}_{id}$ denote the desired acceleration, desired velocity, and desired position, respectively; $\mathbf{F}_{ei}\in\Re^{m_i}$ denotes the interaction force of the i th task.

The reference acceleration for the impedance control can be designed as

$$\ddot{\mathbf{x}}_i^{\,*}=\ddot{\mathbf{x}}_{id}+\mathbf{\Lambda}_{id}^{-1}[\mathbf{B}_{id}(\dot{\mathbf{x}}_{id}-\dot{\mathbf{x}}_i)+\mathbf{K}_{id}(\mathbf{x}_{id}-\mathbf{x}_i)-\mathbf{F}_{ei}]. \quad (20)$$

1) Relation to the Position Control: When a task is performed in free-space, the interaction force is zero, and (20) is reduced to the well-known reference acceleration of the position control,

$$\ddot{\mathbf{x}}_i^{\,*}=\ddot{\mathbf{x}}_{id}+\mathbf{K}_{Vi}(\dot{\mathbf{x}}_{id}-\dot{\mathbf{x}}_i)+\mathbf{K}_{Pi}(\mathbf{x}_{id}-\mathbf{x}_i) \quad (21)$$

with

$$\mathbf{K}_{Vi}=\mathbf{\Lambda}_{id}^{-1}\mathbf{B}_{id} \text{ and } \mathbf{K}_{Pi}=\mathbf{\Lambda}_{id}^{-1}\mathbf{K}_{id}. \quad (22)$$

2) Relation to the Force Control: Equation (20) can be reduced to a reference acceleration of the implicit force control [18]. Let $\mathbf{x}_e$ denote the position of the environment. When a robot contacts with the stiff environment, $\mathbf{x}_{id}$ and $\mathbf{K}_{id}$ can determine[2] the desired interaction force, $\mathbf{F}_{eid}$, as follows:

$$\begin{aligned}\mathbf{K}_{id}(\mathbf{x}_{id}-\mathbf{x}_i)&\approx\mathbf{K}_{id}(\mathbf{x}_{id}-\mathbf{x}_e)\\&=\mathbf{F}_{eid}\end{aligned}. \quad (23)$$

Substituting (23) into (20) leads to the reference acceleration for the implicit force control,

$$\ddot{\mathbf{x}}_i^{\,*}=\ddot{\mathbf{x}}_{id}+\mathbf{K}_{Vfi}(\dot{\mathbf{x}}_{id}-\dot{\mathbf{x}}_i)+\mathbf{K}_{Pfi}(\mathbf{F}_{eid}-\mathbf{F}_{ei}) \quad (24)$$

with

$$\mathbf{K}_{Vfi}=\mathbf{\Lambda}_{id}^{-1}\mathbf{B}_{id} \text{ and } \mathbf{K}_{Pfi}=\mathbf{\Lambda}_{id}^{-1}. \quad (25)$$

D. Dynamic consistency

The dynamic decoupling property is defined as that the joint torque for the task with the lower priority does not produce any operational acceleration of the task with the higher priority [4], [5].

[1] Compliant control is often desirable in many new robotic systems that are supposed to be operated safely in human environment [9].

[2] The contact environment is modeled as a simple spring [20].

Proposition 1. *Suppose that TDE perfectly estimates* $\hat{\mathbf{H}}_{i|prev(i)}$. *Then, the OSFTDE has the dynamical decoupling property.*

Proof. When combining the robot dynamics equation with the controller, we obtain

$$\bar{\mathbf{A}}\ddot{\mathbf{q}}+\mathbf{H}=\sum_{j=1}^{i}\mathbf{J}_{j|prev(j)}{}^T\mathbf{F}_j+\underbrace{\sum_{j=i+1}^{k}\mathbf{J}_{j|prev(j)}{}^T\mathbf{F}_j}_{torques\ with\ the\ lower\ priority}. \quad (26)$$

For the simplicity, assume that the control forces for the i th task and for the tasks with the higher priority consist of only the TDE term as

$$\mathbf{F}_j=\hat{\mathbf{H}}_{j|prev(j)}, \text{ for } 1\le j\le i, \quad (27)$$

and the velocity product terms, $\dot{\mathbf{J}}_i\dot{\mathbf{q}}$ or $\dot{\mathbf{J}}_{i|prev(i)}\dot{\mathbf{q}}$, are ignored.

Multiplying $\mathbf{J}_i\bar{\mathbf{A}}^{-1}$ on both sides of (26), we obtain

$$\begin{aligned}\ddot{\mathbf{x}}_i+\mathbf{J}_i\bar{\mathbf{A}}^{-1}\mathbf{H}=&\underbrace{\mathbf{J}_i\bar{\mathbf{A}}^{-1}\sum_{j=1}^{i}\mathbf{J}_{j|prev(j)}{}^T\hat{\mathbf{H}}_{j|prev(j)}}_{TDE\ term}\\&+\underbrace{\mathbf{J}_i\bar{\mathbf{A}}^{-1}\sum_{j=i+1}^{k}\mathbf{J}_{j|prev(j)}{}^T\mathbf{F}_j}_{acceleration\ from\ the\ force\ with\ the\ lower\ priority}\end{aligned}. \quad (28)$$

Since TDE is assumed to be perfect, TDE term on the right-hand side of (28) is derived as

$$\begin{aligned}&\mathbf{J}_i\bar{\mathbf{A}}^{-1}[\sum_{j=1}^{i}\mathbf{J}_{j|prev(j)}{}^T\hat{\mathbf{H}}_{j|prev(j)}]\\&=\mathbf{J}_i\bar{\mathbf{A}}^{-1}[\sum_{j=1}^{i}\mathbf{J}_{j|prev(j)}{}^T(\mathbf{J}_{j|prev(j)}{}^{\bar{\mathbf{A}}+})^T\mathbf{H}]. \quad (29)\\&=\mathbf{J}_i\bar{\mathbf{A}}^{-1}\mathbf{H}\end{aligned}$$

Then, the TDE term, (29), linearizes the closed-loop dynamics, (28), as follows:

$$\ddot{\mathbf{x}}_i=\underbrace{\mathbf{J}_i\bar{\mathbf{A}}^{-1}\sum_{j=i+1}^{k}\mathbf{J}_{j|prev(j)}{}^T\mathbf{F}_j}_{acceleration\ from\ the\ force\ with\ the\ lower\ priority}. \quad (30)$$

From (7), the right-hand side of (30) becomes

$$\begin{aligned}\mathbf{J}_i\bar{\mathbf{A}}^{-1}\sum_{j=i+1}^{k}\mathbf{J}_{j|prev(j)}{}^T\mathbf{F}_j&=\sum_{j=i+1}^{k}\mathbf{J}_i\bar{\mathbf{A}}^{-1}\mathbf{J}_{j|prev(j)}{}^T\mathbf{F}_j\\&=\sum_{j=i+1}^{k}(\mathbf{J}_i\bar{\mathbf{A}}^{-1}\mathbf{N}_{prev(j)}{}^T)\mathbf{J}_j{}^T\mathbf{F}_j, \quad (31)\\&=\mathbf{0}\end{aligned}$$

Hence, the control forces for the tasks with the lower priority do not generate any acceleration of the i th task. □

Remark 1. Under finite time-delay L, the estimation error of TDE scheme, named by the TDE error, is inevitable [11]-[14]. The TDE error of the i th task, $\mathbf{\varepsilon}_i\in\Re^{m_i}$, is defined as follows:

$$\mathbf{\varepsilon}_i=\bar{\mathbf{\Lambda}}_{i|prev(i)}{}^{-1}(\hat{\mathbf{H}}_{i|prev(i)}-\mathbf{H}_{i|prev(i)}). \quad (32)$$

Then, the TDE error is involved in (30) as follows:

$$\ddot{\mathbf{x}}_i=\mathbf{\varepsilon}_i \quad (33)$$

Hence, the OSFTDE realizes *near* dynamic consistency under finite time-delay L. Although TDE has the inherent limitation, the TDE error, we claim that TDE more accurately and easily enables the dynamic decoupling property than direct usage of robot dynamics models in the face of modeling error. This is to be validated in the following chapter III, and chapter IV.

III. Comparison with the OSF

The OSFTDE is to be compared with the OSF through simulations in two regards: robustness for the modeling error of the inertia and computational efficiency.

The OSF is given as follows [2], [3]:

$$\boldsymbol{\Gamma} = \mathbf{J}_1^T \mathbf{F}_1 + \mathbf{J}_{2|prev(2)}^T \mathbf{F}_2 + \cdots + \mathbf{J}_{k|prev(k)}^T \mathbf{F}_k \text{, and} \quad (34)$$

$$\begin{aligned} \mathbf{F}_i = {} & \hat{\boldsymbol{\Lambda}}_{i|prev(i)}(\mathbf{q})(\ddot{\mathbf{x}}_i^* - \ddot{\mathbf{x}}_{i\_bias}) + \hat{\boldsymbol{\mu}}_{i|prev(i)}(\mathbf{q},\dot{\mathbf{q}}) \\ & + \hat{\mathbf{p}}_{i|prev(i)}(\mathbf{q}) + \hat{\boldsymbol{\eta}}_{i|prev(i)}(\mathbf{q},\dot{\mathbf{q}}) + \mathbf{F}_{\mathbf{e}i|prev(i)} \end{aligned}, \quad (35)$$

where

$$\hat{\boldsymbol{\Lambda}}_{i|prev(i)}(\mathbf{q}) = [\mathbf{J}_{i|prev(i)} \hat{\mathbf{A}}^{-1} \mathbf{J}_{i|prev(i)}^T]^{-1},$$

$$\hat{\boldsymbol{\mu}}_{i|prev(i)}(\mathbf{q},\dot{\mathbf{q}}) = (\mathbf{J}_{i|prev(i)}^{\hat{\mathbf{A}}+})^T \mathbf{b}(\mathbf{q},\dot{\mathbf{q}}) - \hat{\boldsymbol{\Lambda}}_{i|prev(i)}(\mathbf{q}) \dot{\mathbf{J}}_{i|prev(i)} \dot{\mathbf{q}},$$

$$\hat{\mathbf{p}}_{i|prev(i)}(\mathbf{q}) = (\mathbf{J}_{i|prev(i)}^{\hat{\mathbf{A}}+})^T \mathbf{g}(\mathbf{q}),$$

$$\hat{\boldsymbol{\eta}}_{i|prev(i)}(\mathbf{q},\dot{\mathbf{q}}) = (\mathbf{J}_{i|prev(i)}^{\hat{\mathbf{A}}+})^T \mathbf{f}(\mathbf{q},\dot{\mathbf{q}}),$$

$$\mathbf{F}_{\mathbf{e}i|prev(i)} = (\mathbf{J}_{i|prev(i)}^{\hat{\mathbf{A}}+})^T \mathbf{J}_i^T \mathbf{F}_{\mathbf{e}i}, \quad (36)$$

and

$$\mathbf{N}_{prev(i)} = \mathbf{I} - \sum_{j=1}^{i-1} \mathbf{J}_{j|prev(j)}^{\hat{\mathbf{A}}+} \mathbf{J}_{j|prev(j)}. \quad (37)$$

The differences of two control laws, the OSF and the OSFTDE, are summarized as follows: 1) the OSFTDE introduces TDE terms while the OSF uses explicit dynamic models, 2) for the inertia model, the OSFTDE uses a constant nominal model, $\bar{\mathbf{A}}$, while the OSF uses time-varying estimate, $\hat{\mathbf{A}}(\mathbf{q})$.

A. Robustness for the Modeling Error of Inertia

Now, to compare the robustness for the modeling error of inertia, consider the example [3]: the orientation task is performed in the null space of end-effector's (x, y) position. The 3-DOF planar robot manipulator was used in this simulation as illustrated in Fig. 1. Each link has 0.5 m length and 1.0 kg mass.

1) Dynamic Consistency: If the orientation task dynamics is decoupled with the dynamics of the end-effector's (x, y) position, then the control force for the orientation task should not affect the end-effector's (x, y) position.

Typical non-dynamical-consistent control, based on pseudo-inverse of Jacobians, showed large deviation of end-effector's (x, y) position due to the dynamic coupling as shown in Fig. 2(a). Without modeling error of inertia, the

[3] The example is a modified version of the one originally devised in [21].

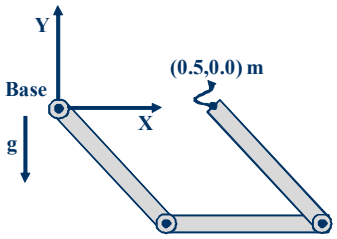

Fig. 1. Initial position of a 3 DOFs planar robot. Each link has 0.5 m length, and 1.0 kg mass. The orientation of the end-effector is controlled in the null space of end-effector's (x,y) position.

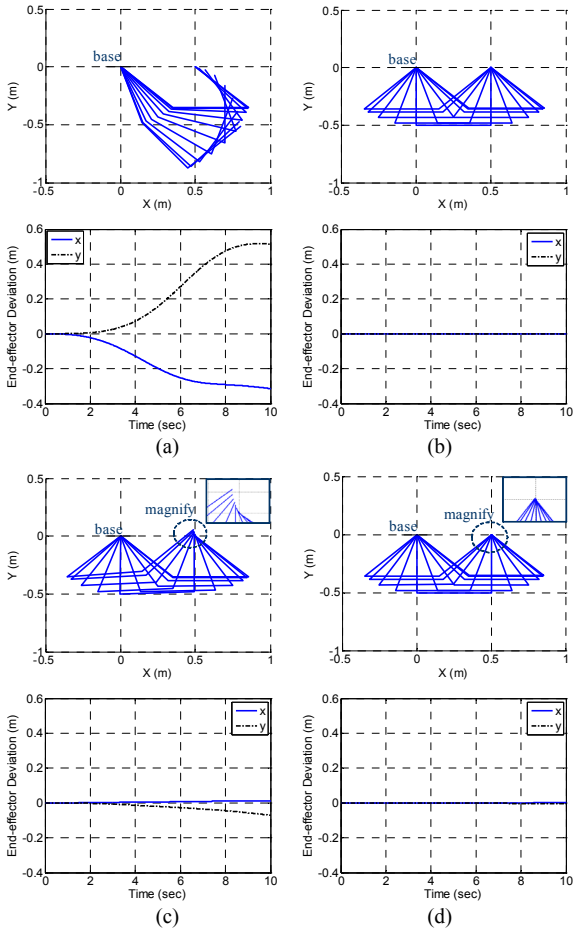

Fig. 2. Comparison of the dynamic consistency: (a) pseudo-inverse method, (b) the OSF without modeling error, (c) the OSF under 5% modeling error, (d) the OSFTDE under 5% modeling error. The inaccurate inertia contaminates the dynamic decoupling property in the OSF. In contrast, the OSFTDE achieves relatively robust dynamic decoupling under the same amount of the modeling error.

OSF perfectly achieved the dynamic decoupling property as shown in Fig. 2(b). However, under 5 % the modeling error of inertia, the dynamic decoupling property of the OSF is contaminated so that relatively large deviation of the end-effector's (x, y) position occurred as shown in Fig. 2(c). In contrast, the OSFTDE realized relatively accurate dynamic decoupling property under the same amount of modeling error in inertia as shown in Fig. 2(d).

2) Control Performance: Let us compare the control accuracy of the orientation task. The simulation results are shown in Fig. 3 and summarized in Table I. Under the same

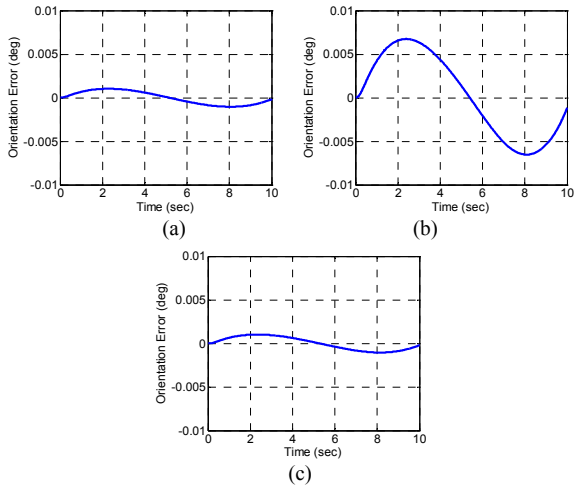

Fig. 3. Comparison of the orientation-task error: (a) the OSF without modeling error, (b) the OSF under 5% modeling error of inertia, (c) the OSFTDE under 5% modeling error of inertia. The modeling error of inertia degrades the control accuracy in the OSF, while the OSFTDE shows good control accuracy under the same amount of the modeling error.

TABLE I
COMPARISON OF THE SIMULATION RESULTS

Controller	Max. deviation of end-effector's position	Max. tracking error of orientation-task
OSF	0.0110 m	0.0067 deg
OSFTDE	0.0019 m	0.0010 deg

The results are obtained under 5% modeling error of inertia.

amount of modeling error in inertia, the OSFTDE showed 15% tracking error of the OSF.

B. Computational Efficiency

The computational efficiency of the OSFTDE was compared with the OSF by examining the required computational effort to evaluate control torque. The computational effort is measured in terms of FLoating point OPerations (FLOPs) that denotes total number of the four arithmetical operations [22].

For the sake of simplicity, assume that all tasks require the same m DOFs. The comparison of computational effort is first generalized in terms of m and n in Table II, and a simulated result is displayed in Fig. 4. The results show that the OSFTDE has about three times better computational efficiency than the OSF.

The difference of the computational effort mainly comes from TDE scheme as follows:

1) The OSF requires the explicit computation of $\hat{\mathbf{A}}(\mathbf{q})$, and $[\hat{\mathbf{b}}(\mathbf{q},\dot{\mathbf{q}})+\hat{\mathbf{g}}(\mathbf{q})]$ that take computational cost $O(n^2)$ [8]. In contrast, the OSFTDE saves this computation but requires the TDE terms, $(\mathbf{F}_{i(t-L)}-\bar{\mathbf{\Lambda}}_{i|prev(i)}\ddot{\mathbf{x}}_{i|prev(i)(t-L)})$, that take $O(m^2)$ (generally, $m<<n$). Note that $\mathbf{F}_{i(t-L)}$ and $\ddot{\mathbf{x}}_{i|prev(i)(t-L)}$ are already computed in the previous step.

2) Also, the OSF needs to compute $\hat{\mathbf{A}}(\mathbf{q})^{-1}$ on-line that takes computational cost $O(n^3)$ [8], [10]. In OSFTDE, however, the expensive computation can be saved since the inverse of constant nominal model of inertia, $\bar{\mathbf{A}}^{-1}$, can be obtained off-line.

3) Finally, the OSF needs to differentiate the task-consistent Jacobians for $\dot{\mathbf{J}}_{i|prev(i)}\dot{\mathbf{q}}$. However, the OSFTDE does not require the explicit computation of $\dot{\mathbf{J}}_{i|prev(i)}\dot{\mathbf{q}}$ since it is implicitly estimated by TDE.

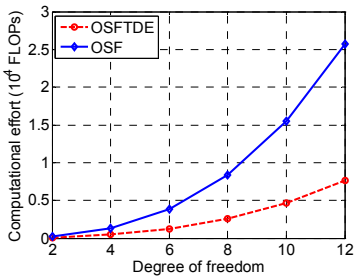

Fig. 4. Comparison of the computational effort for evaluating the control torque in one sampling time as the DOFs increases from 2 to 12 for 2 tasks.

TABLE II
COMPUTATIONAL EFFORT FOR EVALUATING CONTROL TORQUE

	Computational Effort (FLOPs)
OSF	$0.7n^3+[(7k-3)m+0.5k+1.5]n^2$ $+(4km^2+10km+0.5k-0.5)n+km^3+3km^2-km$
OSFTDE	$[(7k-3)m+0.5k-0.5]n^2$ $+[4km^2+2km-0.5(k+1)]n+km^3+3km^2+2km$

The computational effort for an inversion of n by n matrix is approximated as $0.7n^3$ [22].

IV. CONCLUSION

The OSF was enhanced with TDE in practical aspects: robustness for the modeling error and computational efficiency. TDE provides an accurate estimate of nonlinear robot dynamics so that the robot dynamics is linearized with a known value of inertia. By virtue of TDE, dynamic decoupling property is realized under the modeling error of inertia and robust control performance is obtained. Also, TDE saves expensive computations: inversion of inertia, explicit computation of dynamics models, and differentiation of Jacobians. Through simple but obvious simulation, the practical advantages of the proposed control were demonstrated.

The proposed control can be immediately applied to control of high-DOFs robots such as humanoids. Further experiments with 2-DOFs robot manipulator are to be performed. Also, the effect of the TDE error on the dynamic consistency appears to deserve further investigations.

REFERENCES

[1] O. Khatib, "A unified approach for motion and force control of robot manipulators: The operational space formulation," *IEEE J. Robot. Autom.*, vol. RA-3, no. 1, pp. 43–53, Feb. 1987.

[2] O. Khatib, L. Sentis, J. Park and J. Warren, "Whole-body dynamic behavior and control of human-like robots," *Int. Jnl. of Humanoid Robotics*, vol. 1, no. 1, pp. 29-43, 2004.
[3] L. Sentis and O. Khatib, "Prioritized multi-objective dynamics and control of robots in human environments," in *Proc. 4th IEEE/RAS Int. Conf. Humanoid Robots*, Nov. 2004, vol. 2, pp. 764–780.
[4] O. Khatib, "Inertial Properties in Robotic Manipulation: An Object-Level Framework," *Int. J. Robot. Res.*, vol. 13, no. 1, pp. 19-36, 1995.
[5] Roy Featherstone, and Oussama Khatib, "Load Independence of the Dynamically Consistent Inverse of the Jacobian Matrix," *Int. J. Robot. Res.*, vol. 16, no. 2, pp. 19-36, 1997.
[6] Vincent De Sapio, Oussama Khatib, and Scott Delp,"Task-level approaches for the control of constrained multibody systems," *Multibody Syst. Dyn.*, vol. 16, no. 1, pp. 73-102, 2006.
[7] Micaël Michelin, Philippe Poignet, and Etienne Dombre, "Dynamic task/posture decoupling for minimally invasive surgery motions: simulation results," " in *Proc. IEEE/RSJ Int. Conf. Intell. Robots Syst.*, Oct., pp. 3625–3630, 2004.
[8] Jun Nakanishi, Rick Cory, Michael Mistry, Jan Peters and Stefan Schaal, "Operational Space Control: A Theoretical and Empirical Comparison," *Int. J. Robot. Res.*, vol. 27, no. 6, pp. 737-757, 2008.
[9] Jan Peters, and Stefan Schaal, "Learning to control in operational space," *Int. J. Robot. Res.*, vol. 27, no. 2, pp. 197-212, 2008.
[10] Kyong-Sok Chang, and Oussama Khatib, "Efficient recursive algorithm for the operational space inertia matrix of branching mechanisms," *Advanced robotics*, vol. 14, no. 8, pp. 703-715, 2001.
[11] K. Youcef-Toumi and Osamu Ito, "A time delay controller for systems with unknown dynamics", *Trans. of ASME, J. Dyn. Sys., Meas., Contr.*, vol. 112, No. 1, pp. 133-142, 1990.
[12] K. Youcef-Toumi and S. T. Wu, "Input/output linearization using time delay control," *Trans. ASME J. Dyn. Syst. Meas. Control*, vol. 114, no. 1, pp. 10–19, 1992.
[13] T. C. Hsia, "A new technique for robust control of servo systems," *IEEE Trans. Ind. Electron.*, vol. 36, no. 1, pp. 1–7, Feb. 1989.
[14] T. C. Hsia, T. A. Lasky, and Z. Guo, "Robust independent joint controller design for industrial robot manipulators," *IEEE Trans. Ind. Electron.*, vol. 38, no. 1, pp. 21–25, Feb. 1991.
[15] P. Baerlocher and R. Boulic, "Task-priority formulations for the kinematic control of highly redundant articulated structures," in *Proc. IEEE/RSJ Int. Conf. Intell. Robots Syst.*, Oct., pp. 323–329, 1998.
[16] G. F. Franklin, J. Powell, and M. Workman, *Digital Control of Dynamic Systems*. Reading, MA: Addison-Wesley, 1998.
[17] N. Hogan, "Impedance control: An approach to manipulator, parts I-III," *Trans. of ASME, J. Dyn. Sys., Meas., Contr.*, vol. 107, pp. 1-24, 1985.
[18] S. P. Chan and H. C. Liaw, "Generalized impedance control of robot for assembly tasks requiring compliant manipulation," *IEEE Trans. Ind. Electron.,* vol. 43, no. 4, pp. 453-461, Aug. 1996.
[19] Ganwen Zeong, and Ahmad Hemami, "An overview of robot force control," *Robotica*, vol. 15, pp. 473-482, 1997.
[20] Jaeheung Park, and Oussama Khatib, "Robot multiple contact control," *Robotica*, vol. 26, pp. 667-677, 2008.
[21] Oussama Khatib, "Motion/force redundancy of manipulators," *Japan-USA symposium on flexible automation*, pp. 337-342, 1990.
[22] Gene H. Golub and Charles F. Van Loan, *Matrix Computations*, 3rd ed.: Johns Hopkins, 1996.
[23] Sang Hoon Kang, Maolin Jin, and Pyung Hun Chang, "A solution to the accuracy/robustness dilemma in impedance control," *IEEE Trans. Mechatron.*, vol. 14, no. 3, pp. 282-294, 2009.
[24] H. Gariner, M. Mensler, and A. Richard, "Continuous-time model identification from sampled data: implementation issues and performance evaluation," *Int. J. Control*, vol. 76, no. 13, pp. 1337-1357, 2003.
[25] T. Söderström, and P. Stoica, "Instrumental variable methods for system identification," *Circuits, Systems, and Signal Processing*, vol. 21, no. 1, pp. 1-9, 2002.